Real-time diagrammatic Monte Carlo for nonequilibrium quantum transport

Marco Schiró[1] and Michele Fabrizio[1,2]
[1]*International School for Advanced Studies (SISSA) and CRS Democritos, CNR-INFM, Via Beirut 2-4, I-34014 Trieste, Italy*
[2]*The Abdus Salam International Centre for Theoretical Physics (ICTP), P.O. Box 586, I-34014 Trieste, Italy*
(Received 16 January 2009; published 13 April 2009)

We propose a numerically exact approach to nonequilibrium real-time dynamics that is applicable to quantum impurity models coupled to biased noninteracting leads, such as those relevant to quantum transport in nanoscale devices. The method is based on a diagrammatic Monte Carlo sampling of the *real-time* perturbation theory along the Keldysh contour. We benchmark the method on a noninteracting resonant-level model and, as a first nontrivial application, we study zero-temperature nonequilibrium transport through a vibrating molecule.

DOI: 10.1103/PhysRevB.79.153302 PACS number(s): 73.63.−b, 71.27.+a, 74.20.Mn

Recent advances in nanotechnology have made it possible to contact microscopic quantum objects with metallic electrodes. Artificial atoms (quantum dots), molecules, or quantum wires have been contacted, opening several routes toward promising nanoelectronic devices.[1,2] Following the first discovery of the Kondo effect in quantum dots,[3] data have appeared where, e.g., single molecules[4,5] or coupled quantum dots[6] were contacted by metallic leads. These developments raised several physical questions, which make electron transport through nanosystems one of the frontier fields in condensed-matter physics. Contacting microscopic objects is intriguing as it addresses quantum transport in a regime where the tunneling rate may become comparable or even lower relative to other energy scales, such as the electron-electron repulsion or the energy of atomic displacements, a situation which may lead to novel nonequilibrium effects.[7,8]

This experimental progress calls for the development of efficient nonperturbative theoretical tools to treat out-of-equilibrium phenomena. The simplest way to model nonequilibrium transport in nanodevices is through a quantum impurity model, namely, a set of discrete electronic levels a (with creation operators $c^{\dagger}_{a\sigma}$, σ being the spin) mimicking a quantum dot or a molecule, coupled to two baths of noninteracting electrons (the leads, with creation operators $f^{\dagger}_{k\sigma\alpha}$), labeled by some quantum number k. When the two leads ($\alpha=L,R$) are kept at different chemical potentials $\mu_L-\mu_R=eV$, the general Hamiltonian can be written as

$$\mathcal{H}=\sum_{\alpha=L,R}\sum_{k\sigma}\epsilon_{k\alpha}f^{\dagger}_{k\sigma\alpha}f_{k\sigma\alpha}+\mathcal{H}_{\rm loc}[c^{\dagger}_{a\sigma},c_{a\sigma}]+\sum_{ka\alpha\sigma}(V_{ka\alpha}f^{\dagger}_{k\sigma\alpha}c_{a\sigma}+\text{H.c.}). \quad (1)$$

The local Hamiltonian $\mathcal{H}_{\rm loc}$ accounts for all of the physics within the quantum impurity, including strong correlations and possible vibrational degrees of freedoms. It could in principle, because of the discrete set of levels, be diagonalized exactly. However, hybridization to the reservoirs makes the problem hard except in simple cases. Furthermore, the finite bias voltage, which drives the system out of equilibrium, rules out the possibility of applying to this problem all the powerful tools developed during recent decades for equilibrium quantum impurities.[9–11] This problem could be circumvented by the trick proposed in Ref. 12, which however requires a delicate analytic continuation and is only valid for the steady state. Standard many-body approaches to nonequilibrium are usually based on Keldysh perturbation theory and are limited to lowest orders or to partial resummations of an arbitrarily chosen subclass of diagrams.[13–15] While several results have been obtained by these methods, there is still a need of numerical exact approaches to access the most interesting intermediate-coupling regime. However among the recently proposed algorithms dealing with nonequilibrium real-time dynamics, most of them suffer from systematic errors that limit their range of applicability. The iterative real-time path-integral method[16] requires, for instance, both a truncation in the quantum dynamics (Trotter error) but also a long-time cutoff on the correlation induced by the leads, the latter preventing access to the low-bias and low-temperature regime. The path-integral Monte Carlo approach proposed in Ref. 17, while treating exactly the lead degrees of freedom, still relies on a time discretization. The time-dependent extension of numerical renormalization group (NRG) (Ref. 18) allows for an accurate description of the equilibrium real-time dynamics. However, its extension to dissipative nonequilibrium dynamics at finite bias is questionable because of the finite size of the leads, corresponding to the maximum number of NRG iterations, even if some progress has been recently achieved for the steady state.[19]

In this work we present a *numerically exact* approach to nonequilibrium dynamics in quantum impurity models, which is based on a diagrammatic Monte Carlo[11] (diagMC) sampling of the real-time Keldysh perturbation theory in the hybridization Hamiltonian. The method is *numerically exact* since it does not require any discretization in the quantum dynamics or in the size of the fermionic reservoirs. These features make our scheme particularly well suited to describe transient dynamics and dissipation in open quantum systems within a completely unbiased approach. We benchmark the method on a noninteracting resonant-level model at zero temperature. Then, as a first application, we compute the inelastic tunneling spectrum of a resonant level coupled to a local vibrational mode.

Formulation. To set up the method, we consider an initially decoupled system, made by the isolated impurity and by the two leads, each assumed to be at equilibrium with its own reservoir at chemical potential μ_α. At time $t=0$, we switch on hybridization in Eq. (1) and let the system evolve with the full Hamiltonian $\mathcal{H}$. Given an initial density matrix,

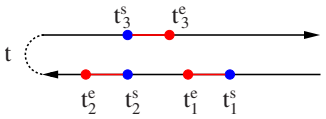

FIG. 1. (Color online) Example of a configuration with $k=3$ segments, each starting at t_i^s and ending at t_i^e, $i=1,2,3$. Here blue (dark gray)/red (gray) dots stands for annihilation/creation operators of the initially occupied level while red segments indicate how the vertices are connected by the hybridization functions $\Delta_{\mathcal{K}}(t^e,t^s)$ in the particular configuration shown. Arrows indicate time-ordering operation along the contour.

ρ_0, we want to compute average values of physical operators evolved in real time from 0 to $t>0$. Real-time quantum dynamics can be represented as an evolution along the so-called Keldysh contour $\mathcal{K}$, plotted in Fig. 1, made of two branches winding around the real-time axis from zero to t (lower branch) and back from t to zero (upper branch). Then, the average value of any operator $\mathcal{O}$ can be written as

$$\langle \mathcal{O}(t)\rangle = \mathrm{Tr}\left(\rho_0 T_{\mathcal{K}}\left\{\exp\left[-i\int_{\mathcal{K}} d\tau \mathcal{H}(\tau)\right]\mathcal{O}\right\}\right), \tag{2}$$

where the trace is over the lead and impurity degrees of freedom, and $T_{\mathcal{K}}$ denotes time ordering along the Keldysh contour. The main idea of our approach is to expand evolution operator (2) in powers of the hybridization and trace out exactly the lead degrees of freedom. The resulting diagrams are then sampled with a Monte Carlo algorithm which looks like the natural generalization to the Keldysh contour of the diagrammatic Monte Carlo method of Ref. 11. To show how the method works, we start by considering a spinless biased resonant-level model (RLM), namely, a single fermionic energy level ε_d driven out of equilibrium by an applied bias $eV=\mu_L-\mu_R$ between the two leads. Given an initial density matrix $\rho_0=\rho_{\mathrm{leads}}\otimes\rho_{\mathrm{imp}}$, with ρ_{leads} describing the two uncoupled leads and ρ_{imp} an initially occupied impurity, we are interested in computing, for example, the real-time evolution of the RLM population $n=c^\dagger c$. Expanding Keldysh evolution operator (2) in powers of the hybridization and tracing out the degrees of freedom of the leads, we get

$$\begin{aligned}\langle n(t)\rangle = \sum_{k=0}^{\infty}\sum_{n=0}^{k}(-1)^k \int_0^{t_k^s} dt_k^e \int_0^{t_{k-1}^e} dt_k^s \ldots \\ \times \int_0^{t_{k-n}^s} dt_{k-n}^e \int_0^{t} dt_{k-n}^s \int_0^{t} dt_{k-n-1}^e \\ \times \int_0^{t_{k-n-1}^e} dt_{k-n-1}^s \ldots \int_0^{t_2^s} dt_1^e \int_0^{t_1^e} dt_1^s \\ \times \mathcal{D}_k(t_1^e,\ldots,t_k^e|t_1^s,\ldots,t_k^s)\mathcal{L}_k(t_1^e,\ldots,t_k^e|t_1^s,\ldots,t_k^s).\end{aligned} \tag{3}$$

Here $\mathcal{D}_k$ results from tracing the lead degrees of freedom. It can be expressed in closed form as the determinant of a $k\times k$ matrix $\mathcal{M}^{-1}$,

$$\mathcal{D}_k(t_1^e,\ldots,t_k^e|t_1^s,\ldots,t_k^s) = \det(\mathcal{M}^{-1}), \tag{4}$$

whose entries are the Keldysh hybridization functions

$$\mathcal{M}_{ij}^{-1} = \Delta_{\mathcal{K}}(t_i^e,t_j^s)s(t_i^e,t_j^s), \tag{5}$$

which we define as

$$\Delta_{\mathcal{K}}(t^e,t^s) = \sum_{k\alpha}|V_{k\alpha}|^2\langle T_{\mathcal{K}}[f_{k\alpha}(t^e)f_{k\alpha}^\dagger(t^s)]\rangle. \tag{6}$$

We adopt the standard definition of the Keldysh Green's functions, namely, we consider t^s, t^e as living on the contour $\mathcal{K}$. We note the additional sign $s(t^e,t^s)$, which is negative when the two times are on opposite branches and positive otherwise. While the determinant $\mathcal{D}_k$ properly accounts for the effects associated to the leads, the function $\mathcal{L}_k$ involves only the impurity degrees of freedom and can be generally written as an average over the initial impurity density matrix, namely,

$$\mathcal{L}_k = \langle T_{\mathcal{K}}[c^\dagger(t_k^e)c(t_k^s)\ldots c^\dagger(t_1^e)c(t_1^s)n(t)]\rangle_{\mathrm{imp}}. \tag{7}$$

Algorithm. The expansion thus obtained admits a natural representation in terms of a collection of k segments, $t\in[t_i^s,t_i^e]$, or equivalently $k-1$ antisegments, $t\in[t_i^e,t_{i+1}^s]$, properly ordered along the contour $\mathcal{K}$ and connected in all possible ways by the Keldysh hybridization functions $\Delta_{\mathcal{K}}(t^e,t^s)$. An example of such a configuration for $k=3$ is plotted in Fig. 1. Each configuration contributes to the sum with its own weight, which is given here by $\mathcal{D}_k$. We sample the whole configuration space using a Monte Carlo procedure. Three basic updates are implemented: adding/removing a segment, adding/removing an antisegment, or shifting a segment endpoint. We accept or reject a new configuration according to a detailed balance prescription. In the actual simulation, we store and update the matrix $\mathcal{M}$ defined in Eq. (5), which is the only quantity required to compute Metropolis acceptance ratios.[11]

Benchmark. We benchmark the method on the biased spinless RLM. Its nonequilibrium real-time dynamics, despite being analytically solvable by standard methods, has proven to be very difficult to access within other numerical approaches,[16,17] especially in at low bias and low temperature, where the correlations induced by the fermionic leads decay slower than exponential in time. To test the reliability of our method, we compute the occupation number $\langle n(t)\rangle$ at zero temperature as a function of time t and for different values of the level position ε_d, both in equilibrium, $eV=0$, as well as out of equilibrium, $eV\neq 0$, and compare the exact results with diagMC data. In this simple case, we expect that a single energy scale, namely, the level broadening $\Gamma=\pi\Sigma_k|V_k|^2\delta(\varepsilon_k)$, will control the approach to the steady state. As can be seen in Fig. 2, the diagMC calculation perfectly matches the exact solution. We are able to resolve both the short-time transient after the initial configuration and the approach to steady state. A finite applied bias $eV\neq 0$ cuts off Keldysh evolution operator (2) (the steady state is reached earlier than at $eV=0$), as pointed out by Ref. 20, thus making the expansion more convergent. Moreover, within the present approach we can easily measure the current flow through the impurity $I(t)=\frac{1}{2}\langle I_L(t)-I_R(t)\rangle$ on a fine real-time grid in a very efficient way. Results shown in Fig. 2 confirm that a true *nonequilibrium* steady state with a finite value of the current is reached at long times due to the infinite size of the bath.

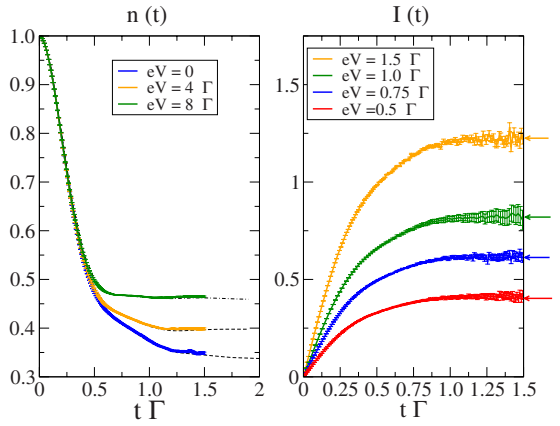

FIG. 2. (Color online) Zero-temperature real-time dynamics for different bias values eV of the dot population, $\langle n(t)\rangle$, from an initially occupied dot (left panel) and of the current, $\langle I(t)\rangle$ (right panel) of the resonant-level model. DiagMC results (dots) are compared with the exact solution (full line). We take $\epsilon_d=\Gamma$ and consider a flat density of states in the leads with a half bandwidth 10Γ. The increasing error bars for larger times is due to the limited simulation time.

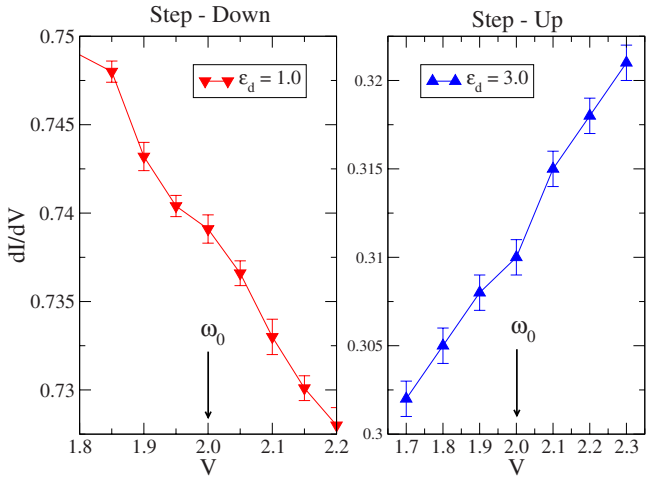

FIG. 3. (Color online) Zero-temperature differential conductance dI/dV (in unit of e^2/h) for bias values eV around $\omega_0=2.0\Gamma$. Electron-phonon coupling is $g=0.5\omega_0$. We consider two different values of the fermionic level position ε_d in order to reproduce the crossover from reduced (step-down) to enhanced (step-up) conductance.

Dissipation occurs entirely within the fermionic reservoir and we do not need to include any fictitious bosonic bath to reach a steady state.[17] A delicate issue to discuss when sampling real-time quantum dynamics is the so-called sign problem, namely, the exponential scaling of relative statistical errors in the Monte Carlo estimate of any observable in the infinite-size limit. In this respect, the main advantage of the diagrammatic Monte Carlo method is that one pointed out in Ref. 21: both the thermodynamic limit as well as the zero-temperature/zero-bias limit can be safely taken with no numerical effort while the computational demanding part is related to the long-time limit because the average number of sampled diagrams scales roughly linearly in time. While for the simple RLM model we can reach the steady state running the code for a couple of days on a laptop, when an exponentially small energy scale in the tunneling controls the physics, as, e.g., in the Kondo regime, *ad hoc* resummation,[21] or more efficient sampling criteria must be used to improve accuracy.

Nonequilibrium transport through a single molecule. As a first nontrivial application we consider a simple model of a molecular conductor, namely, a spinless fermionic level coupled to Holstein phonons. The local Hamiltonian is

$$\mathcal{H}_{\rm loc}(n)=\frac{\omega_0}{2}(x^2+p^2)+gx\left(n-\frac{1}{2}\right)+\varepsilon_d\left(n-\frac{1}{2}\right), \qquad (8)$$

where g is the electron-phonon coupling, ω_0 is the phonon frequency (x is the phonon displacement and p its conjugate momentum), ε_d is the energy of the level, and n its occupancy. Our Keldysh diagMC can be naturally extended to include local phonons,[22] the only difference appearing in the trace over local degrees of freedom (7), now involving fermionic operators time evolved according to Hamiltonian (8) for the electron-phonon subsystem. This trace can be evaluated analytically by observing that the local Hamiltonians with different level occupancy $n=0,1$ are related one to the other by a unitary transformation, $\mathcal{H}_{\rm loc}(0)+\epsilon_d=U^\dagger\mathcal{H}_{\rm loc}(1)U$, with $U=\exp(igp/\omega_0)$. It follows that the bosonic contribution to the local trace reduces the following bosonic correlation function

$$\mathcal{L}_k^{\rm ph}={\rm Tr}[\rho_{\rm ph}U^\dagger(t_k^e)U(t_k^s)U^\dagger(t_{k-1}^e)\ldots U(t_1^s)], \qquad (9)$$

which can be easily evaluated analytically for most common initial phonon density matrices $\rho_{\rm ph}$, which we assume the equilibrium distribution at zero temperature. In Eq. (9) $U(t)$ and $U^\dagger(t)$ are the unitary operators evolved with $\mathcal{H}_{\rm loc}(1)$, and we have assumed the level initially occupied. The coupling to molecular vibrations is known to significantly affect inelastic electron tunneling.[23] When the bias hits a vibrational frequency, the differential conductance dI/dV changes sharply. Experimentally, it is observed that dI/dV increases in the tunneling regime but decreases in the opposite case of a high transmission barrier. Although simple physical arguments can be invoked[24,25] to explain this phenomenon, theoretical calculations have so far been restricted to lowest orders in the electron-phonon coupling.[26,27] In the simple resonant-level model that we are considering, previous perturbative calculations predicted that dI/dV at bias $eV=\omega_0$ should decrease or increase if the zero-bias conductance $G>0.5$ or $G<0.5$, respectively, in units of the unitary value (in our spinless case e^2/h). Evidences for this were very recently reported by Tal and co-workers[8] with H_2O molecules bridging a Pt break junction. Since the Keldysh diagMC is nonperturbative in the electron-phonon coupling, it offers the possibility to verify these perturbative predictions. We model the two regimes of $G\gtrless 0.5$ by two different values of the level position $\varepsilon_d=1$ and 3, the former closer to resonance than the latter, and compute directly the differential conductance dI/dV. As can be seen from Fig. 3, either step-down or step-up features do appear around the threshold for

vibronic excitations, $eV \simeq \omega_0$, when the zero-bias conductance is greater or lower than 0.5, respectively, in agreement with perturbative results.[26,27] We also note that the step is not as abrupt as in perturbation theory, likely signaling a significant phonon damping.

In summary, we have introduced a numerically exact approach to nonequilibrium quantum transport in nanoscopic conductors. The method is based on a diagrammatic Monte Carlo sampling of the *real-time* perturbation theory in the impurity-lead hybridization, performed along the Keldysh contour required to treat nonequilibrium effects. Our approach is free from any systematic error since it does not require truncating of the real-time dynamics or introduction of finite-size effects in the leads. Moreover, in spite of the oscillating nature of the quantum evolution, we are able to follow the dynamics starting from an arbitrary initial preparation up to the steady state. This is primarily due to the combined effects of infinite leads and of the applied bias, which cut off the Keldysh evolution operator. It is also due to the capability of the algorithm to cope with sign problem. As a first application we studied the zero-temperature nonlinear transport through a simple model molecular conductor. Being completely general, our method can in principle be applied to any discrete quantum system bridging two noninteracting conducting leads, providing a tool to study quantum transport in nanoscopic devices.

Note added: After completion of this work, we became aware of a similar attempt by Schmidt *et al.*,[28] further developed in Ref. 29.

We are grateful to Nikolay Prokof'ev, Erio Tosatti, and Massimo Capone for stimulating discussions and comments. This research was partially supported by MIUR-PRIN Contract No. 2006022847 and CINECA.

[1] N. J. Tao, Nat. Nanotechnol. **1**, 173 (2006).
[2] G. Cuniberti, G. Fagas, and F. Richter, *Introducing Molecular Electronics* (Springer, Berlin, 2005).
[3] D. Goldhaber-Gordon, J. Göres, M. A. Kastner, H. Shtrikman, D. Mahalu, and U. Meirav, Phys. Rev. Lett. **81**, 5225 (1998).
[4] H. Park, J. Park, A. K. L. Lim, E. H. Anderson, A. P. Alivisatos, and P. L. McEuen, Nature (London) **407**, 57 (2000).
[5] J. J. Parks, A. R. Champagne, G. R. Hutchison, S. Flores-Torres, H. D. Abruna, and D. C. Ralph, Phys. Rev. Lett. **99**, 026601 (2007).
[6] E. A. Stinaff, M. Scheibner, A. S. Bracker, I. V. Ponomarev, V. L. Korenev, M. E. Ware, M. F. Doty, T. L. Reinecke, and D. Gammon, Science **311**, 636 (2006).
[7] S.-F. Shi, K. I. Bolotin, F. Kuemmeth, and D. C. Ralph, Phys. Rev. B **76**, 184438 (2007).
[8] O. Tal, M. Krieger, B. Leerink, and J. M. van Ruitenbeek, Phys. Rev. Lett. **100**, 196804 (2008).
[9] R. Bulla, T. A. Costi, and T. Pruschke, Rev. Mod. Phys. **80**, 395 (2008).
[10] A. N. Rubtsov, V. V. Savkin, and A. I. Lichtenstein, Phys. Rev. B **72**, 035122 (2005).
[11] P. Werner, A. Comanac, L. de' Medici, M. Troyer, and A. J. Millis, Phys. Rev. Lett. **97**, 076405 (2006).
[12] J. E. Han and R. J. Heary, Phys. Rev. Lett. **99**, 236808 (2007).
[13] H. Schoeller and J. König, Phys. Rev. Lett. **84**, 3686 (2000).
[14] A. Rosch, J. Paaske, J. Kroha, and P. Wolfe, J. Phys. Soc. Jpn. **74**, 118 (2005).
[15] A. Oguri, J. Phys. Soc. Jpn. **74**, 110 (2005).
[16] S. Weiss, J. Eckel, M. Thorwart, and R. Egger, Phys. Rev. B **77**, 195316 (2008).
[17] L. Mühlbacher and E. Rabani, Phys. Rev. Lett. **100**, 176403 (2008).
[18] F. B. Anders and A. Schiller, Phys. Rev. Lett. **95**, 196801 (2005).
[19] F. B. Anders, Phys. Rev. Lett. **101**, 066804 (2008).
[20] A. Mitra, I. Aleiner, and A. J. Millis, Phys. Rev. Lett. **94**, 076404 (2005).
[21] N. Prokof'ev and B. Svistunov, Phys. Rev. Lett. **99**, 250201 (2007).
[22] P. Werner and A. J. Millis, Phys. Rev. Lett. **99**, 146404 (2007).
[23] M. Galperin, M. Ratner, and A. Nitzan, J. Phys.: Condens. Matter **19**, 103201 (2007).
[24] R. C. Jaklevic and J. Lambe, Phys. Rev. Lett. **17**, 1139 (1966).
[25] B. Persson, Phys. Scr. **38**, 282 (1988).
[26] M. Paulsson, T. Frederiksen, H. Ueba, N. Lorente, and M. Brandbyge, Phys. Rev. Lett. **100**, 226604 (2008).
[27] R. Egger and A. O. Gogolin, Phys. Rev. B **77**, 113405 (2008).
[28] T. L. Schmidt, P. Werner, L. Mühlbacher, and A. Komnik, Phys. Rev. B **78**, 235110 (2008).
[29] P. Werner, T. Oka, and A. J. Millis, Phys. Rev. B **79**, 035320 (2009).